

## LYMPHOID NEOPLASIA

## ATM deficiency promotes development of murine B-cell lymphomas that resemble diffuse large B-cell lymphoma in humans

Karen S. Hathcock,<sup>1</sup> Hesed M. Padilla-Nash,<sup>2</sup> Jordi Camps,<sup>2,3</sup> Dong-Mi Shin,<sup>4,5</sup> Daniel Triner,<sup>1</sup> Arthur L. Shaffer III,<sup>6</sup> Robert W. Maul,<sup>7</sup> Seth M. Steinberg,<sup>8</sup> Patricia J. Gearhart,<sup>7</sup> Louis M. Staudt,<sup>6</sup> Herbert C. Morse III,<sup>4</sup> Thomas Ried,<sup>2</sup> and Richard J. Hodes<sup>1,9</sup>

<sup>1</sup>Experimental Immunology Branch, <sup>2</sup>Genetics Branch, National Cancer Institute, National Institutes of Health, Bethesda, MD; <sup>3</sup>Gastrointestinal and Pancreatic Oncology Group, Institut D'Investigacions Biomèdiques August Pi i Sunyer, Centro de Investigación Biomédica en Red de Enfermedades Hepáticas y Digestivas, Barcelona, Spain; <sup>4</sup>Laboratory of Immunopathology, National Institute of Allergy and Infectious Diseases, National Institutes of Health, Bethesda, MD; <sup>5</sup>Department of Food and Nutrition, Seoul National University, Seoul, Korea; <sup>6</sup>Lymphoid Malignancies Branch, National Cancer Institute, National Institutes of Health, Bethesda, MD; <sup>7</sup>Laboratory of Molecular Biology and Immunology, National Institute on Aging, National Institutes of Health, Bethesda, MD; <sup>8</sup>Biostatistics and Data Management Section, Office of the Clinical Director, National Cancer Institute, National Institutes of Health, Bethesda, MD; and <sup>9</sup>National Institute on Aging, National Institutes of Health, Bethesda, MD

## Key Points

- ATM deficiency promotes the development of murine B-cell lymphomas that model human ABC DLBCL.
- T cell–dependent immune surveillance may be important to prevent emergence of ATM-deficient B-cell lymphomas.

The serine-threonine kinase ataxia-telangiectasia mutated (ATM) plays a central role in maintaining genomic integrity. In mice, ATM deficiency is exclusively associated with T-cell lymphoma development, whereas B-cell tumors predominate in human ataxia-telangiectasia patients. We demonstrate in this study that when T cells are removed as targets for lymphomagenesis and as mediators of immune surveillance, ATM-deficient mice exclusively develop early-onset immunoglobulin M<sup>+</sup> B-cell lymphomas that do not transplant to immunocompetent mice and that histologically and genetically resemble the activated B cell–like (ABC) subset of human diffuse large B-cell lymphoma (DLBCL). These B-cell lymphomas show considerable chromosomal instability and a recurrent genomic amplification of a 4.48-Mb region on chromosome 18 that contains *Malt1* and is orthologous to a region similarly amplified in human ABC DLBCL. Of importance, amplification of *Malt1* in these lymphomas correlates with their dependence on nuclear factor (NF)- $\kappa$ B, MALT1, and B-cell

receptor (BCR) signaling for survival, paralleling human ABC DLBCL. Further, like some human ABC DLBCLs, these mouse B-cell lymphomas also exhibit constitutive BCR-dependent NF- $\kappa$ B activation. This study reveals that ATM protects against development of B-cell lymphomas that model human ABC DLBCL and identifies a potential role for T cells in preventing the emergence of these tumors. (*Blood*. 2015;126(20):2291-2301)

## Introduction

Ataxia-telangiectasia mutated (ATM) is a serine-threonine kinase that communicates between molecules that sense DNA double-strand breaks and downstream effector mechanisms that are necessary to maintain genomic integrity.<sup>1</sup> ATM primarily functions to coordinate cellular responses to double-strand breaks by phosphorylating key proteins that initiate activation of DNA damage checkpoints, leading to cell cycle arrest, DNA repair, or apoptosis. Consequently, when ATM is deficient, cellular responses to DNA damage are defective, and genomic integrity is not maintained. Humans with mutations in *ATM* develop the autosomal recessive disease ataxia-telangiectasia (A-T). ATM-deficient mice exclusively develop T-cell lymphomas,<sup>2,3</sup> whereas B-cell malignancies outnumber T-cell malignancies in human A-T patients.<sup>4,5</sup> Although these findings demonstrate that ATM is required to prevent T-cell transformation in mice, they fail to explain why other malignancies are rarely seen. To determine whether ATM plays a role in

preventing transformation of non-T-cell lineages, we generated ATM-deficient mice (ATM knockout [KO]) that also lacked T cells (CD3 $\epsilon$ -deficient, CD3 $\epsilon$ KO). Strikingly, ATM- and T cell–deficient mice (ATMKO.CD3 $\epsilon$ KO) develop early-onset B-cell lymphomas that resemble human activated B cell–like (ABC) diffuse large B-cell lymphoma (DLBCL).

DLBCLs are highly prevalent and compose 25% of all human lymphoid malignancies. This is a heterogeneous disease that can be subdivided into 2 main lymphoma categories, germinal center (GC) B cell–like (GCB) and ABC, which differ in their gene expression profiles and clinical outcomes.<sup>6–12</sup> In addition, ABC DLBCL, but not GCB DLBCL, depends on constitutively active nuclear factor (NF)- $\kappa$ B for survival.<sup>11,13,14</sup> Because ABC DLBCL is more clinically aggressive and less responsive to therapeutic interventions, models of this disease would be useful.

Submitted June 27, 2015; accepted September 19, 2015. Prepublished online as *Blood* First Edition paper, September 23, 2015; DOI 10.1182/blood-2015-06-654749.

The data reported in this article have been deposited in the Gene Expression Omnibus database (accession numbers GSE68505 and GSE59578).

The online version of this article contains a data supplement.

The publication costs of this article were defrayed in part by page charge payment. Therefore, and solely to indicate this fact, this article is hereby marked “advertisement” in accordance with 18 USC section 1734.

The study presented here extends the requirement for ATM in preventing T-cell lymphomas to include a role for ATM in also preventing murine B-cell lymphomas. In addition, we identify a previously unappreciated role for T cells in protection against these B-cell lymphomas. Gene expression profiling demonstrates a striking similarity between mouse ATMKO.CD3εKO B-cell lymphomas and human ABC DLBCL. These mouse lymphomas contain a recurrent genomic amplification of a region on chromosome 18 (MMU18) containing *Malt1*<sup>11,15</sup> in the region of highest amplification and orthologous to an amplification that has been identified in human ABC DLBCL.<sup>7,9</sup> Of importance, the presence of amplified *Malt1* in these lymphomas correlates with their dependence on NF-κB,<sup>11,13</sup> MALT1,<sup>14,16</sup> and B-cell receptor (BCR)<sup>17</sup> signaling for survival, paralleling human ABC DLBCL, and providing a model to study this disease.

## Materials and methods

### Mice

ATMKO.CD3εKO and ATMKO mice were generated on mixed B6 × 129 backgrounds by parallel breeding of ATM<sup>+/-</sup>.129<sup>3</sup> with CD3εKO<sup>18</sup> and C57BL/6 mice, respectively. Activation-induced cytidine deaminase (AID)-deficient mice were generated by interbreeding ATM<sup>+/-</sup>.CD3εKO mice and AIDKO.CD3εKO mice.<sup>19</sup> Mouse studies were performed at the Frederick Cancer Research Facility (Frederick, MD), following protocols approved by the National Cancer Institute and the Frederick Cancer Research Facility Institutional Animal Care and Use Committee.

### Cell lines

In vitro cultures of B- and T-lymphoma cell lines were established from spleens (ATMKO.CD3εKO) and thymi (ATMKO), respectively, of tumor-bearing mice using published methods but without interleukin-2 addition.<sup>3</sup>

### Microarray-based gene expression profiling

Total RNA was labeled and applied to 2-color whole-mouse genome microarrays (Agilent Technologies) according to the manufacturer's protocols. RNA was prepared from splenic B cells (ATM wild-type [WT] and KO) treated with or without goat-anti-mouse-immunoglobulin (Ig)M, GC B cells (ATMWT), and B-cell lymphomas. For gene expression analysis after Bruton tyrosine kinase (BTK) inhibition, tumor samples treated with PCI-32765 (Cy5) were compared to samples treated with dimethylsulfoxide (DMSO) (Cy3). Expression data (Cy5/Cy3 ratios) were extracted using Agilent Technologies Feature Extraction software (version 9.1) and analyzed as previously described.<sup>20</sup> Raw data were normalized with the limma package in R (<http://www.r-project.org/>). Differentially expressed genes were identified with significance analysis of microarrays (<http://statweb.stanford.edu/~tibs/SAM/>) with 1% false discovery rate. Data presented here have been deposited in the National Center for Biotechnology Information's Gene Expression Omnibus database,<sup>21</sup> GEO Series accession number GSE68505.

### Metaphase preparation and SKY

Metaphase spreads were prepared according to standard protocols and incubated with spectral karyotyping (SKY) probes prepared as described previously.<sup>22,23</sup> Imaged metaphase spreads were analyzed using nomenclature and ploidy rules established for mouse chromosomes (<http://www.informatics.jax.org/mgihome/nomen/anomalies.shtml>).<sup>24</sup>

### Array CGH

Oligonucleotide-based array comparative genomic hybridization (CGH) was conducted on mouse genome CGH microarray (Agilent Technologies) as described previously.<sup>25</sup> Scanned images were analyzed using the rank segmentation and the genomic identification of significant targets in cancer (GISTIC)

algorithms within the Nexus Copy Number software version 7.5 (BioDiscovery). Data presented here were deposited in the National Center for Biotechnology Information's Gene Expression Omnibus,<sup>21</sup> GEO Series accession number GSE59578.

### NF-κB immunofluorescence

Cells were cultured overnight on poly-D-lysine-coated dishes (MatTek), fixed in 4% paraformaldehyde (Electron Microscopy Sciences), and permeabilized with 0.5% Triton X-100. Cells were stained with anti-Rel (sc-71; Santa Cruz Biotechnology) and Alexa488-conjugated secondary antibody (A11070; Molecular Probes, Life Technologies). Nuclei were counter-stained with 50 nM 4,6-diamidino-2-phenylindole (Molecular Probes, Life Technologies).

### In vitro cell inhibition experiments

Reagents tested for inhibitory effects on lymphoma cell recovery include PS1145 (inhibitor of NF-κB [IKK] inhibitor) (Sigma-Aldrich), MLN120B (IKK inhibitor) (ChemScene), Z-VPRPR-fmk (MALT1 caspase inhibitor) (Enzo Life Sciences), MI-2 (MALT1 inhibitor) (Xcess Biosciences), PRT2667 (Syk inhibitor) (gift of Dr Ryan M. Young, National Cancer Institute), PCI-32765 (BTK inhibitor) (ChemieTek), and Ly317615 (protein kinase C [PKC]β inhibitor) (Axon Medchem). Viable cells were counted using trypan blue exclusion, and percentage inhibition was presented relative to DMSO as [(cell number in DMSO well – cell number in test well) ÷ (cell number in DMSO well)] × 100.

### Western blot analysis

Lymphoma cells were treated with PCI-32765 or DMSO at 37°C, and lysates were prepared as described previously,<sup>26</sup> with addition of sodium orthovanadate (Sigma-Aldrich) and Phosphatase Inhibitor Cocktail 3 (Sigma-Aldrich). Antibodies used include anti-phospho-Ser32-IkBα (p-IkBα) (14D4; Cell Signaling Technology), anti-IkBα (44D4; Cell Signaling Technology), and anti-β-actin (Ac-15; Sigma). Primary antibodies were detected with anti-rabbit immunoglobulin-horseradish peroxidase (Cell Signaling Technology) or anti-mouse immunoglobulin-horseradish peroxidase (Cell Signaling Technology).

## Results

### ATMKO.CD3εKO mice develop early-onset IgM<sup>+</sup> B-cell lymphomas

Because T cell-sufficient ATMKO mice develop thymic lymphomas at high frequency, we generated mice that were both ATM and T-cell deficient (ATMKO.CD3εKO) to determine whether ATM also functions to prevent oncogenic transformation of non-T cells. ATMKO.CD3εKO mice developed enlarged abdomens between 3 and 9 months old, and at necropsy, 63 of 72 mice exhibited splenomegaly and hepatomegaly. Hematoxylin and eosin-stained spleen sections revealed compressed red pulp and greatly expanded white pulp containing large cells that were primarily centroblastic with small prominent nucleoli at the nuclear membrane or that were immunoblastic with large bar-shaped magenta nucleoli, features diagnostic of mouse DLBCL<sup>27</sup> (Figure 1A-C). Immunohistology showed that these cells were B220<sup>+</sup>, confirming their B-cell origin (Figure 1D), and, consistent with T-cell deficiency, GCs were never observed. Enlarged livers were heavily infiltrated with large lymphoid cells having the same cytologic features as in spleen. These studies indicated that when T cells were absent, ATM functioned to prevent transformation of B cells into aggressive lymphomas that histologically resemble DLBCL.

Median age at necropsy of ATMKO.CD3εKO mice with these pathological findings was 5.1 months. In contrast, ATMKO mice on a similar mixed B6 × 129 genetic background but WT for CD3ε and, consequently, T-cell sufficient, died of thymic lymphomas (median

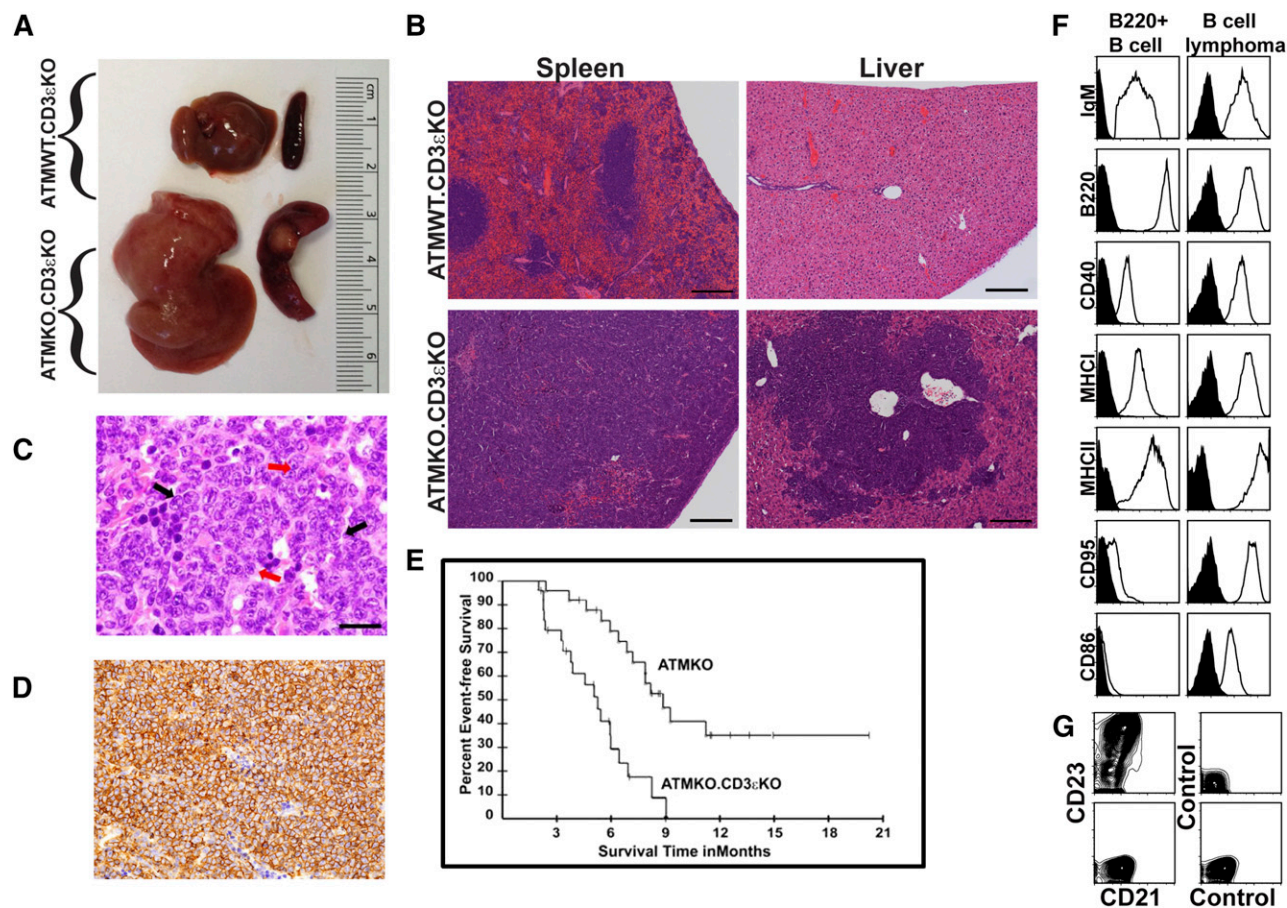


**Figure 1. ATMKO.CD3 $\epsilon$ KO mice develop early-onset B-cell lymphomas in spleen and liver that resemble DLBCL.** (A) Representative image of spleens (right) and livers (left) from ATMWT.CD3 $\epsilon$ KO and ATMKO.CD3 $\epsilon$ KO mice. (B) Hematoxylin and eosin staining showing spleen and liver sections from ATMWT.CD3 $\epsilon$ KO (top) and ATMKO.CD3 $\epsilon$ KO mice (bottom) (original magnification  $\times 10$ ; bar represents 200  $\mu$ m). (C) Hematoxylin and eosin staining of a spleen section prepared from a tumor-bearing ATMKO.CD3 $\epsilon$ KO mouse (original magnification  $\times 1000$ ; bar represents 20  $\mu$ m). Red and black arrows denote centroblasts and immunoblasts, respectively. (D) B220 staining of a spleen section from a tumor-bearing ATMKO.CD3 $\epsilon$ KO mouse (original magnification  $\times 400$ ; bar = 100  $\mu$ m) using 3,3'-diaminobenzidine tetrahydrochloride as chromogen. Images were viewed with an Olympus BX41 microscope and photographed with an Olympus DP71 camera. Dynamic positioning controller software (version 3.3.1.292) was used for image acquisition. (E) The probability of dying with a tumor was determined using the Kaplan-Meier method. Kaplan-Meier analysis of tumor incidence studies in ATMKO.CD3 $\epsilon$ KO ( $n = 25$ ) and ATMKO ( $n = 24$ ) mice. ATMKO.CD3 $\epsilon$ KO mice died with B-cell lymphomas and ATMKO mice died with thymic T-cell lymphomas. No thymic T-cell lymphomas were observed in ATMKO.CD3 $\epsilon$ KO mice and no B-cell lymphomas were detected in ATMKO mice. No ATMWT.CD3 $\epsilon$ KO or ATMWT mice died with lymphomas. Mice euthanized and not found to have either a B- or T-cell tumor had their observations censored in the analysis. (F) Flow cytometric analysis of IgM, B220, CD40, MHC class I (MHCI; K<sup>b</sup>), MHC class II (MHCII; IA<sup>b</sup>), CD95, and CD86 expression (open histogram) or isotype control staining (shaded histogram) on normal splenic B cells (gated on IgM<sup>+</sup> cells) and on 1 representative ATMKO.CD3 $\epsilon$ KO B-cell lymphoma. (G) CD21 and CD23 expression on splenic B220<sup>+</sup> B cells and 1 ATMKO.CD3 $\epsilon$ KO B-cell lymphoma. These histograms are representative of results obtained from 20 individual tumors. Data acquisition was performed using a FACSCaliber flow cytometer (BD Biosciences), and FlowJo software (Tree Star) was used for analysis.

survival, 8.5 months; Figure 1E). Therefore, failure to detect B-cell lymphomas in T-cell-sufficient ATMKO mice was not due to T-cell lymphomas killing mice before B-cell lymphomas develop but rather suggests that T cells play a pivotal role in preventing emergence of these B-cell malignancies.

Flow cytometry demonstrated that ATMKO.CD3 $\epsilon$ KO lymphomas expressed surface markers characteristic of mature activated B cells (Figure 1F). All lymphomas were IgM<sup>+</sup> and expressed B-cell markers (B220 and CD40), as well as high levels of major histocompatibility complex (MHC) class I (K<sup>b</sup>), MHC class II (IA<sup>b</sup>), costimulatory (CD86), and death receptor (CD95) molecules. In addition, they had an unusual CD21<sup>+</sup>CD23<sup>+</sup> phenotype that is shared with T-independent (T-I) memory B cells (Figure 1G).<sup>28</sup>

Sequencing of immunoglobulin heavy chain variable (VH) regions from early passage lymphomas isolated from 6 different mice demonstrated that each was monoclonal and used different V, D, and J genes. Each cell line contained shared VH mutations (present in all or most cells) and unique mutations (present in only a few cells), suggesting

monoclonal origins and ongoing somatic mutation<sup>29</sup> (Table 1; supplemental Figures 2-7, available on the *Blood* Web site). Overall, the frequency of mutations was  $3.5$  to  $8.7 \times 10^{-3}$ /bp, a frequency higher than that detected in activated B cells from AID-deficient mice, but lower than that reported for T-dependent (TD) GC B cells.<sup>30</sup> Consistent with the detection of ongoing VH mutations, quantitative polymerase chain reaction revealed that these lymphomas expressed *Aicda* at levels similar to those detected in lipopolysaccharide-activated normal B cells (supplemental Figure 1).

Because AID has been shown to play an essential role in some models of B-cell lymphomagenesis,<sup>31-33</sup> we compared AID-deficient and -sufficient ATMKO.CD3 $\epsilon$ KO littermates to determine whether AID was required for B-cell tumor development in this model. Fourteen of 22 AIDKO and 43 of 59 AIDWT ATMKO.CD3 $\epsilon$ KO mice died with B-cell lymphomas (median survival, 4.4 and 4.6 months, respectively). Tumor phenotypes were indistinguishable, demonstrating that AID was not required for B-cell lymphomagenesis in this model (supplemental Figure 8).

**Table 1. Mutational analysis of IgM VH regions in ATMKO.CD3εKO B-cell lymphomas**

	Tumor identification no.					
	12437	16508	25787	39317	178119	180764
VDJ	J558.74.176, DFL16.1, JH4	J558.54.148, DST4.2, JH4	Vh10.2b, DSP2.2, JH1	J558.66.165, DSP2.12, JH2	J606.1.79, DFL16.1, JH3	J558.16.106, DSP2.5, JH3
Clones, N (~350 bp per clone)	8	5	6	7	10	4
Mutations, N	13	13	15	8	30	11
Mutation frequency ( $\times 10^{-3}$ )	4.6	8	7	3.5	8.7	8

Each tumor was derived from a different mouse.

**ATMKO.CD3εKO lymphomas stimulate in vitro T-cell responses and undergo in vivo T cell-dependent rejection**

We established in vitro cell lines from enlarged ATMKO.CD3εKO spleens and attempted to propagate these cells by in vivo transfer. Transferred cell lines grew progressively in T cell-deficient CD3εKO mice but not in T cell-sufficient (B6  $\times$  129)F1 mice (the mixed genetic background of ATMKO.CD3εKO lymphomas) (Figure 2A). Consistent with their high levels of expressed MHC and costimulatory molecules (Figure 1F),<sup>34</sup> these lymphomas stimulated vigorous in vitro proliferation of CD4<sup>+</sup> T cells from both (B6  $\times$  129)F1 and allogeneic BALB/c mice (Figure 2B). These results indicate that ATMKO.CD3εKO B-cell lymphomas are immunogenic and provide a possible explanation for their absence in T cell-sufficient ATMKO mice and for their inability to expand when adoptively transferred into T cell-sufficient mice.

**Gene expression profiling of ATMKO.CD3εKO lymphomas reveals similarities to human ABC DLBCL**

To further characterize these B-cell lymphomas, we compared gene expression profiles of 9 cell lines to those of anti-IgM-stimulated primary B cells (ATMKO.CD3εKO and ATMWT.CD3εKO) and GC B cells (ATMWT). The heat map generated by unsupervised clustering of all genes showed that lymphomas and primary mouse B-cell populations have distinct patterns of gene expression (Figure 3), as was reported when gene expression profiling of human primary B cells and DLBCL was performed.<sup>8</sup> We identified clusters of coordinately expressed genes and analyzed these clusters to identify those statistically enriched for gene expression signatures that define specific signaling pathways and differentiation states<sup>35</sup> (supplemental Table 1). Clusters C1 to C3 were associated with high expression in activated B cells and were enriched for pathways that include BCR, cytokine, interferon, and NF-κB signaling. Cluster 1 was generally restricted to BCR activation of primary B cells and was not a feature of GC B cells or our lymphoma cells, whereas cluster 2 was more highly expressed in all primary cells compared to lymphomas. Cluster 3, which was highly expressed in activated B cells and lymphomas but low in GC B cells, was enriched in genes that define the B-cell activation and differentiation states of human ABC DLBCL, namely BCR signaling, NF-κB activation, and plasmacytic differentiation. Cluster 4 was generally higher in GC B cells and enriched for genes associated with metabolic demands of proliferation, such as ribosomal genes. Cluster 5 was also associated with proliferation, but had features of NF-κB signaling and MYC activation, and was most highly expressed in GC B cells and in B cells after 6 hours of activation. Gene expression in cluster 6 was substantially higher in, and specific to, the B-cell tumors and contained genes that define the human ABC DLBCL phenotype, including *Malt1* and *Tcf4*. Lastly, genes that are associated with cell cycle progression during proliferation were upregulated in lymphomas and in GC B cells and were not induced in primary activated B-cell samples.

We next examined genes that were statistically overexpressed or underexpressed in specific cell populations. Genes that were more highly expressed in primary cells than in lymphomas fell into gene

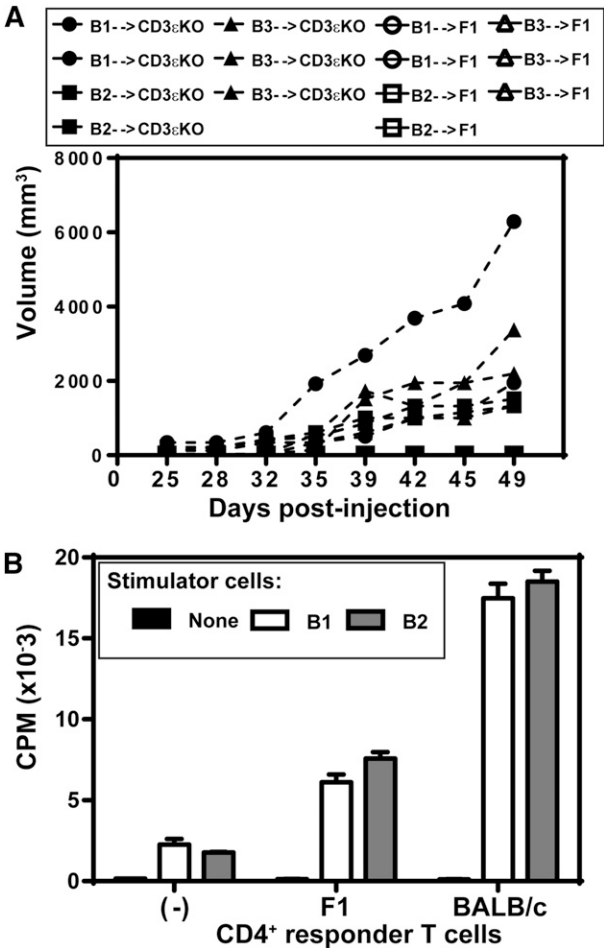
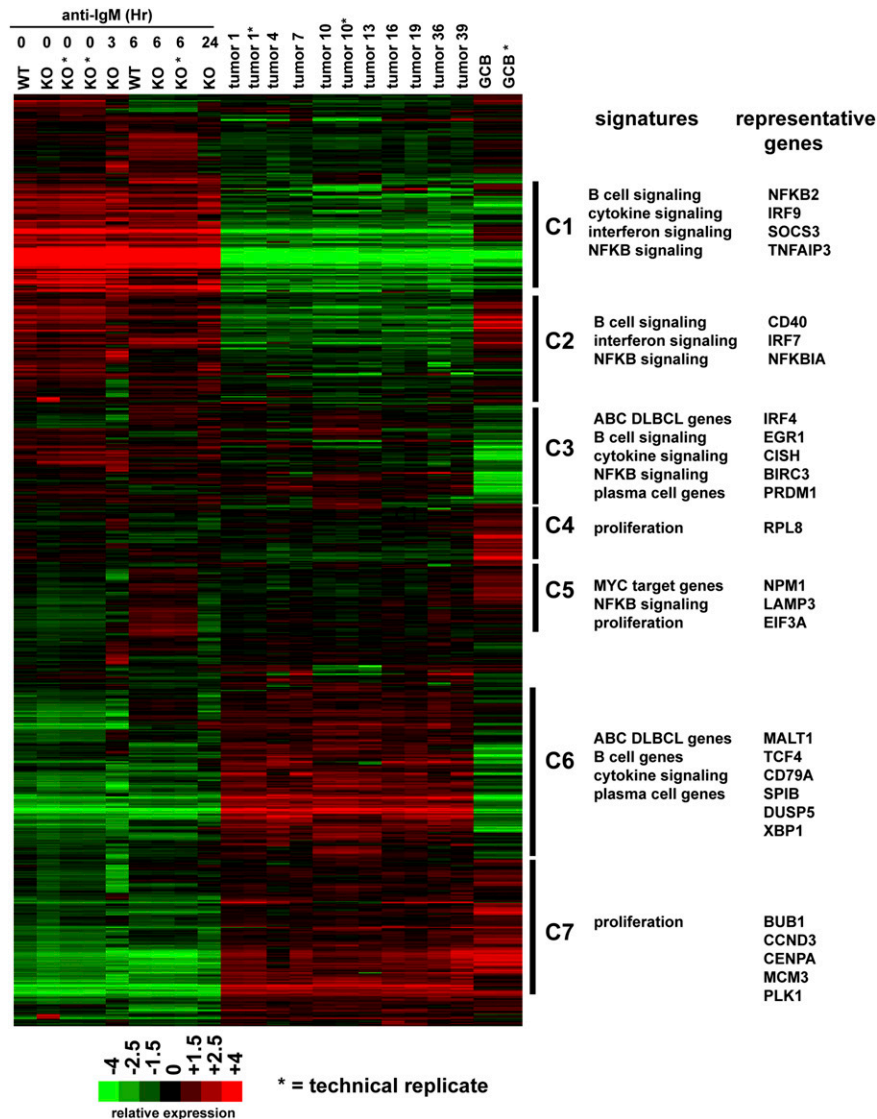


**Figure 2. ATMKO.CD3εKO B-cell tumors activate in vitro T-cell responses and undergo in vivo T cell-dependent rejection.** (A) ATMKO.CD3εKO B-cell tumors grow progressively in T cell-deficient (CD3εKO) (closed symbols), but not in T cell-sufficient (B6  $\times$  129)F1 (F1; open symbols, which are all on the x-axis), host mice. A total of  $2 \times 10^5$  B-cell lymphomas (B1, B2, and B3) were injected in 100  $\mu$ L of phosphate-buffered saline into the anteromedial thigh of host mice, and tumor growth (plotted as tumor volume) was calculated as described in supplemental Materials and Methods. This experiment is representative of 4 independent experiments using 3 B-cell tumors and 2 to 4 host mice per group. (B) ATMKO.CD3εKO B-cell lymphomas stimulate in vitro CD4<sup>+</sup> T-cell proliferation. No T cells (-) or a total of  $1 \times 10^5$  CD4<sup>+</sup> T cells from (B6  $\times$  129)F1 (F1) or BALB/c mice were cocultured with  $1 \times 10^5$  irradiated (60 Gy) B-cell lymphomas (none, B1, or B2) for 72 hours in 96-well plates. T-cell proliferation was assessed by [<sup>3</sup>H] thymidine uptake and presented as counts per minute (CPM)  $\pm$  standard error of the mean for triplicate wells. This experiment is representative of 3 experiments using 2 B-cell tumors.



**Figure 3. Microarray-based gene expression profiling of primary B cells and B-cell lymphomas.** Heat map of RNA gene expression profiles from splenic B cells (ATMWT [WT] and ATMKO [KO]), treated with or without goat-anti-mouse IgM (15  $\mu$ g/mL) stimulation (at 0, 3, 6, and 12 hours), ATMWT GC B cells (GCB), and 9 ATMKO.CD3 $\epsilon$ KO tumors. RNA was labeled with Cy5 and compared to a common pool of reference RNA labeled with Cy3 to allow direct comparison of all samples to each other. Clusters of genes with similar behaviors were identified (supplemental Table 1) and captured for subsequent signature analysis (supplemental Table 2) to identify enriched functions and pathways. Genes representative of a particular function are listed on the right. Relative differences in expression are indicated by the color bar; \* indicates a technical replicate of that sample.



signatures<sup>35,36</sup> that included those defining cytokine (*Jak2*) and interferon signaling (*Irf7* and *Irf9*) (supplemental Table 2). Of interest, ABC DLBCL typically also downmodulates interferon responses to avoid the toxic effects of autocrine/paracrine type I interferon.<sup>37</sup> Genes more highly expressed in GC B cells than in lymphomas were those that define both the GCB phenotype (*Aicda*) and proliferation state (*Cdc6* and *Mdm1*). Genes that were more highly expressed in tumors than in primary cells were again enriched for signatures associated with human ABC DLBCL and included genes sets that define NF- $\kappa$ B signaling (*Irf4*), cytokine signaling (*Il10*), and plasmacytic differentiation (*Xbp1*), as well as genes that distinguish ABC DLBCL from GCB DLBCL (*Tcf4*).

**ATMKO.CD3 $\epsilon$ KO lymphomas exhibit chromosome instability and recurrent amplification of a 4.48-Mb region on MMU18 containing *Malt1* in the region of highest amplification**

SKY<sup>22,23</sup> revealed that both freshly explanted (a mix of lymphoma cells and nontransformed splenocytes) and early-passage lymphomas had near-diploid abnormal karyotypes with chromosomal instability. Cells exhibited chromosomal imbalances and structural aberrations such as deletions, duplications, and unbalanced translocations, whereas

reciprocal translocations, a feature of ATMKO T-cell lymphomas,<sup>3</sup> were rare (Figure 4A-B; supplemental Table 3). Of interest, SKY identified gains at the distal end of MMU18 in 4 of 5 of the day 0 lymphomas and in all (11/11) of the early-passage lymphomas analyzed. This gain resulted primarily from amplifications occurring in the form of homogeneously staining regions or unbalanced translocations involving MMU18.

Array CGH<sup>25</sup> confirmed and extended the SKY results, demonstrating that these lymphomas exhibited high levels of aneuploidy and a recurrent 4.48-Mb common region of high-level genomic amplification at chromosome 18:65,490,103-69,966,590. This MMU18 amplicon was detected in 7 of 9 day 0 cells and was retained in all (11/11) early-passage cells (Figure 4C-F). Gene expression profiling revealed that the majority of genes present in the MMU18 amplicon were found in clusters 6 and 7 (Figure 3) and were associated with high expression in B-cell tumors and with low expression in primary B-cell populations. When expression of these genes was directly examined (Figure 4G), 37 of 38 genes in the amplicon were indeed overexpressed, suggesting that amplification leads to upregulation of genes in this region.

GISTIC,<sup>38</sup> a tool used to identify genes affected by copy number alterations that drive cancer growth, identified a statistically significant peak of amplification within the MMU18 amplicon that mapped to

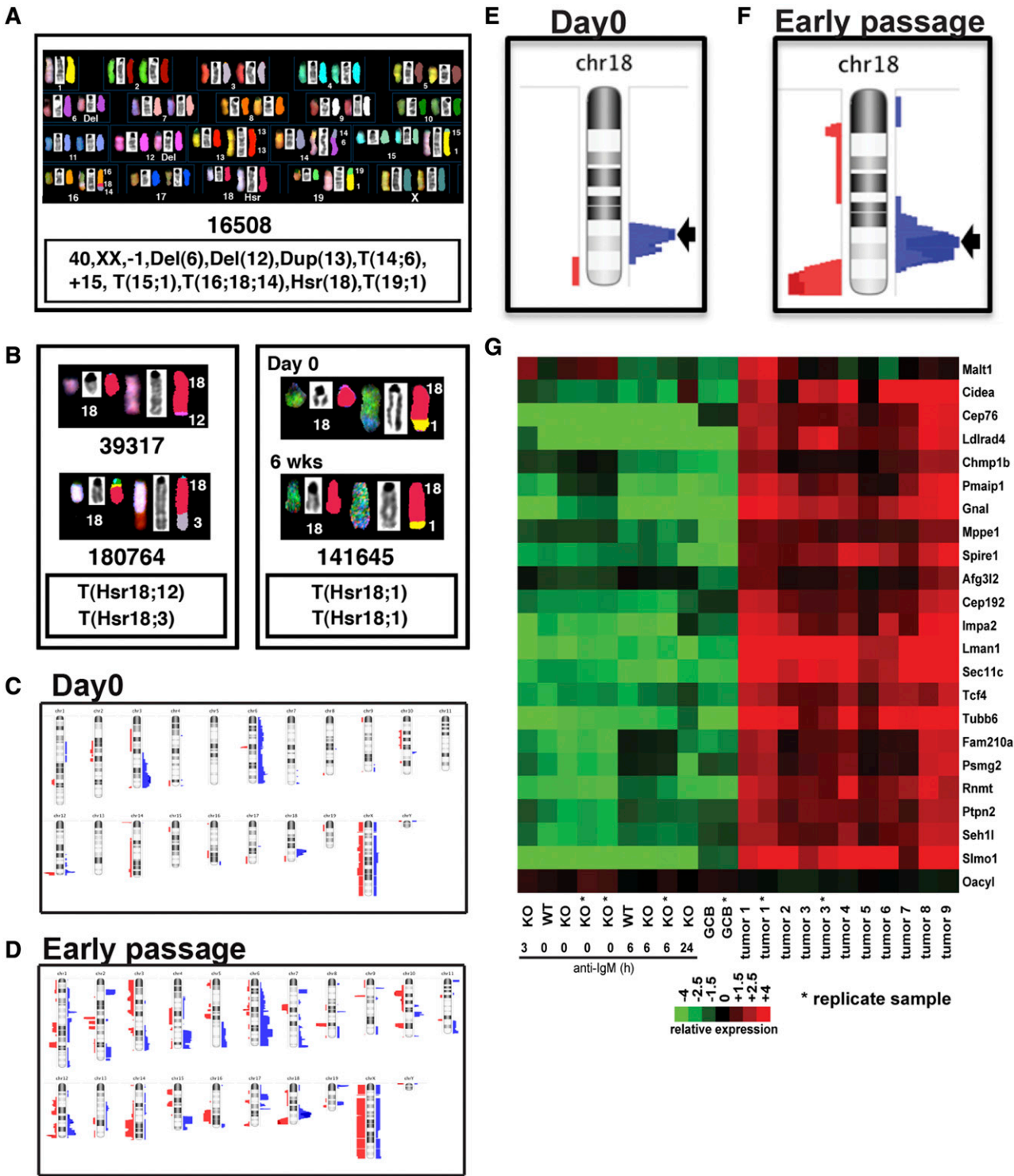


**Figure 4. ATMKO.CD3εKO B-cell lymphomas exhibit chromosomal instability and a gain of a 4.48-Mb region on MMU18.** (A) SKY image of a metaphase chromosome spread prepared from an early-passage (6 weeks) ATMKO.CD3εKO B-cell lymphoma (16508) identifies structural and numerical aberrations, including deletions (MMU6 and MMU12), unbalanced translocations [T(14;6), T(15;1), T(16;18;14), and T(19;1)], and an aberrant MMU18 with an amplified homogeneous staining region (Hsr). (B) SKY images from 3 ATMKO.CD3εKO tumors (39317 and 180764 (left) and 141645 at day 0 and early passage (right) provide examples of structural aberrations that contributed to copy number gains of MMU18 sequences in these tumors. Metaphase images (15 per sample) of day 0 (n = 5) and early-passage tumors (n = 11) were collected at room temperature using a Leica DMRBE epifluorescence microscope fitted with a charge-coupled device camera, a 63× oil-immersion lens, and SpectraCube SD200 acquisition software (Applied Spectral Imaging). Analysis was performed using SKYview software (Applied Spectral Imaging). Array CGH analysis of genome-wide copy number alteration changes in day 0 (n = 9) (C) and early-passage (n = 12) ATMKO.CD3εKO tumors (D) using Nexus Copy Number software (BioDiscovery). Identification of the minimal region of genomic amplification on MMU18 (black arrow) that is present in day 0 (n = 9) (E) or early-passage (n = 12) samples (F). Copy number alteration gains are to the right of the chromosome (blue) and losses are to the left (red). (G) Gene expression profiling from Figure 3 was mined for the expression of genes found in the recurrent amplicon on MMU18 in these B-cell tumors. Relative differences in expression are indicated by the color bar; \* indicates a technical replicate of that sample.

a similar location in day 0 and in cultured lymphoma cells. GISTIC identified a 0.6-Mb minimal region in day 0 cells and a 0.35-Mb region in early-passage cells that mapped to chr18:65,490,103-66,087,220 and chr18:65,490,103-65,840,172, respectively ( $q < 1e-03$ ). Thus, both freshly explanted and cultured ATMKO.CD3 $\epsilon$ KO B-cell lymphomas exhibited aneuploidy and chromosomal instability, with a characteristic MMU18 genomic amplification defined by GISTIC.

We next asked whether genes present in the MMU18 amplicon might contribute to transformation and/or survival. We identified *Malt1* as a candidate for further study because it was the only full-length gene contained within the region identified by GISTIC. In addition, MALT1 links BCR signaling to downstream NF- $\kappa$ B activation<sup>11,39,40</sup> and is known to contribute survival signals to human ABC DLBCL.<sup>14,16</sup> Therefore, we investigated whether B-cell lymphomas were dependent on MALT1 and NF- $\kappa$ B for survival.

### ATMKO.CD3 $\epsilon$ KO lymphomas express activated NF- $\kappa$ B and depend on NF- $\kappa$ B for survival

NF- $\kappa$ B activation begins when inhibitory proteins sequestering inactive NF- $\kappa$ B in the cytoplasm are phosphorylated by activation and subsequently degraded, thereby allowing nuclear translocation of NF- $\kappa$ B proteins.<sup>41</sup> Therefore, as a measure of NF- $\kappa$ B activation, we quantitated relative levels of Rel in the cytoplasm and nucleus by immunofluorescence. Strong Rel staining was observed in both the cytoplasm and the nucleus of B-cell lymphomas (Figure 5A); in contrast, strong Rel staining was detected in the cytoplasm, but not in the nucleus, of control T-cell lymphomas. Correspondingly, the quantified Rel nuclear/cytoplasmic ratio was significantly higher in B-cell tumors than in T-cell tumors (Figure 5B), consistent with NF- $\kappa$ B activation in B-cell lymphomas.

Demonstrating that B-cell lymphomas expressed activated NF- $\kappa$ B prompted us to ask whether they also required NF- $\kappa$ B for survival. Because NF- $\kappa$ B signaling requires IKK activation, we tested NF- $\kappa$ B dependence by assessing viable cell recovery in the presence of either of 2 IKK inhibitors: PS1145<sup>42</sup> or MLN120B<sup>43</sup> (Figure 5C-D). Viable cell recovery of B-cell lymphomas, but not ATMKO T-cell lymphomas, was substantially inhibited by treatment with either agent. Therefore, as assessed by IKK inhibition, these mouse B-cell lymphomas are dependent on NF- $\kappa$ B for viability.

### ATMKO.CD3 $\epsilon$ KO B-cell lymphomas depend on MALT1 activity for survival

We next asked whether *Malt1*, encoded in the recurrent amplicon on MMU18, also contributes to survival of these B-cell lymphomas. Real-time polymerase chain reaction demonstrated that *Malt1* transcript levels were substantially higher in lymphomas than in activated normal B cells (Figure 5E), confirming the results of gene expression profiling presented previously. In vitro recovery of B-cell lymphomas, but not T-cell lymphomas, was substantially inhibited by treatment with either of 2 MALT1 inhibitors: Z-VRPR-fmk<sup>16</sup> or MI-2<sup>44</sup> (Figure 5F-G). These results demonstrate that B-cell lymphomas express elevated levels of *Malt1* and depend on MALT1 activity for their survival, providing an important functional link between *Malt1* gene amplification and the requirement for MALT1 in survival of these B-cell lymphomas.

### Blockade of BCR signaling components impairs survival and suppresses NF- $\kappa$ B activation in ATMKO.CD3 $\epsilon$ KO B-cell lymphomas

For normal and many malignant B cells, BCR signaling provides essential survival signals, in part through MALT1-dependent activation of NF- $\kappa$ B signaling.<sup>11,12,17,39,45-47</sup> As compared to T-cell lymphomas,

cell recovery of B-cell tumors was substantially and preferentially inhibited by in vitro coculture with Syk (PRT2667), BTK (PCI-32765), and PKC $\beta$  inhibitors (Ly317615) (Figure 6A-C). These results demonstrate that survival of ATM-deficient B-cell lymphomas is, at least in part, dependent on Syk, BTK, and PKC $\beta$  signaling and further suggest that they are dependent on BCR signaling for survival.

Because inhibition of BTK signaling impaired survival of ATMKO.CD3 $\epsilon$ KO B-cell lymphomas, we asked whether BTK signaling was also essential for NF- $\kappa$ B activation in these tumors. B-cell lymphomas were treated with PCI-32765 or DMSO, lysed, and subjected to sequential western blot analysis to detect p-IkB $\alpha$  (an indicator of activated NF- $\kappa$ B) and IkB $\alpha$  (a measure of total cellular NF- $\kappa$ B).<sup>48</sup> Decreasing p-IkB $\alpha$ /IkB $\alpha$  ratios were detected beginning as early as 1 hour after PCI-32765 addition (Figure 6D), demonstrating that BTK signaling was required for NF- $\kappa$ B activation in these lymphomas.

Previously, gene expression profiling of a human ABC DLBCL cell line treated with PCI-32765 identified a set of genes that were coordinately downregulated by BTK inhibition.<sup>47</sup> Therefore, we performed gene expression profiling to examine the behavior of these human malignancy-defined genes in ATMKO.CD3 $\epsilon$ KO B cell tumors treated with the BTK inhibitor. These same genes were inhibited in mouse lymphomas (Figure 6E), and there was statistically significant overlap between the genes downregulated by BTK inhibition in human ABC DLBCL cell lines and in mouse lymphomas (supplemental Table 4). NF- $\kappa$ B-dependent genes defined in human ABC DLBCL were also downregulated, thus identifying them as targets for BTK inhibition in these mouse lymphomas as well (Figure 6F; supplemental Table 4). These approaches demonstrate that NF- $\kappa$ B activation in ATMKO.CD3 $\epsilon$ KO B-cell tumors is dependent on BTK signaling and suggest that the effect of inhibiting BTK and/or BCR signaling on cell viability is a consequence of inhibiting downstream NF- $\kappa$ B activation. Activation of NF- $\kappa$ B by BCR signaling is a defining feature of human ABC DLBCL and is strikingly similar in these ATMKO.CD3 $\epsilon$ KO B-cell lymphomas.

## Discussion

We established a mouse model of ATM deficiency in the absence of T cells to explore the extent to which ATM influences development of non-T-cell malignancies. We demonstrate that ATM is required to prevent B-cell lymphomagenesis and identify an unexpected role of T cells in preventing development of these B-cell lymphomas. When T cells are absent, ATM deficiency allows exclusive and early development of clonal B-cell lymphomas that are immunostimulatory and have an array of characteristics that resemble human ABC DLBCL.

Somatic mutations or deletions of *ATM* are observed in sporadic human lymphoid malignancies, including >11% of DLBCLs.<sup>49-52</sup> Although 10% to 15% of all A-T patients develop a spectrum of malignancies, primarily lymphoid, early in life,<sup>4,5,49,53-55</sup> B-cell malignancies are approximately 4 times more frequent than T-cell malignancies<sup>4,5</sup> and only thymic T-cell lymphomas develop in ATM-deficient mice.<sup>3</sup> In contrast to the recurrent translocations involving the T-cell receptor  $\delta$  locus on MMU14 present in ATMKO T-cell lymphomas, no recurrent translocations were identified in the B-cell lymphomas characterized here. The observed differences in translocations involving immune receptor genes between ATM-deficient T- and B-cell tumors may reflect differences in the development stages at which T- and B-cell transformation occurs. That is, T-cell transformation occurs in immature T cells when T-cell receptors are rearranging, whereas these B-cell lymphomas appear to arise from B cells undergoing transformation at a later stage of development, after BCR rearrangement is complete.

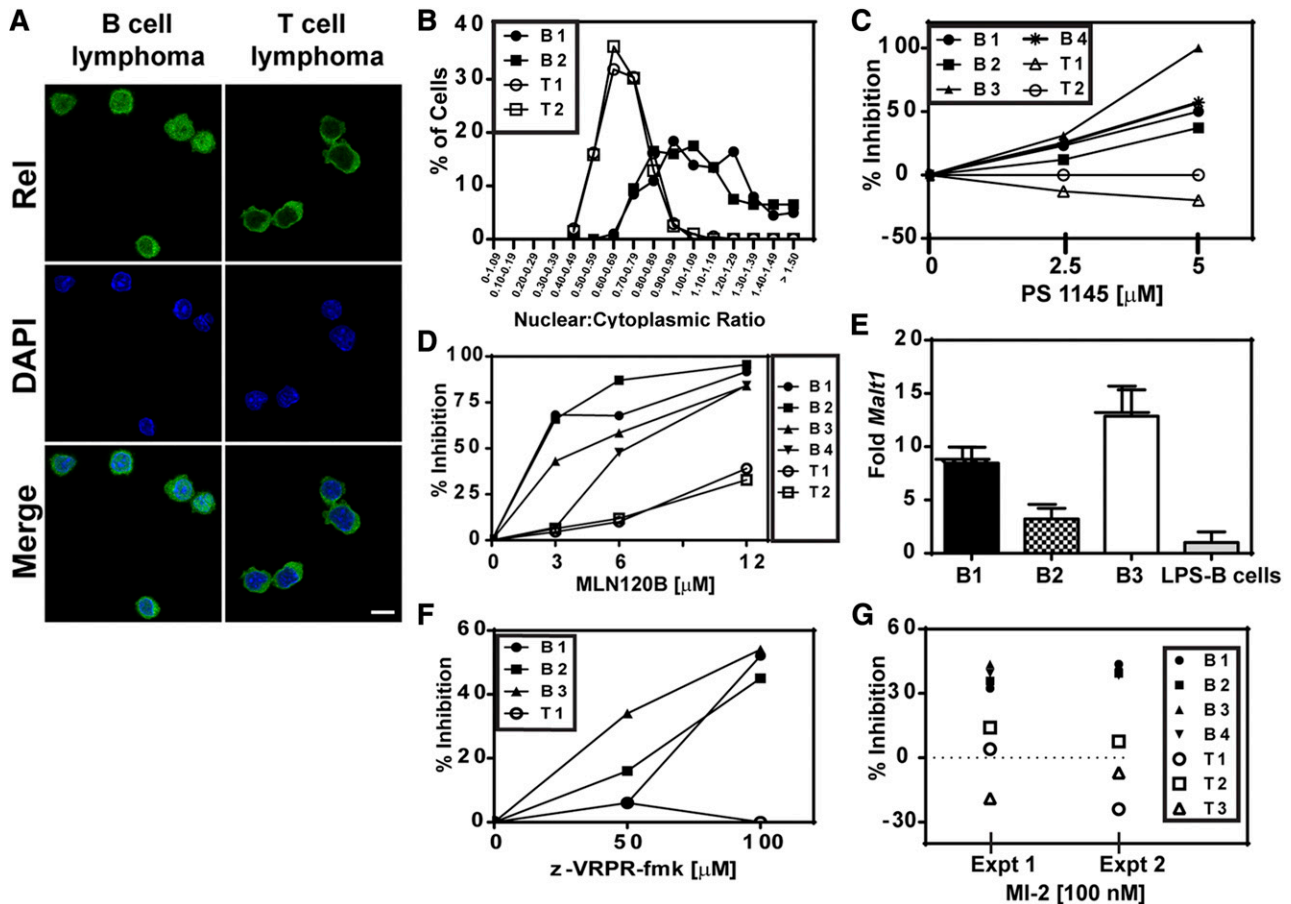


**Figure 5. NF- $\kappa$ B expression and dependence of ATMKO.CD3 $\epsilon$ KO B-cell lymphomas.** (A) Immunofluorescence images showing staining for Rel (Alexa488), 4,6 diamidino-2-phenylindole (DAPI), or both in an ATMKO.CD3 $\epsilon$ KO B-cell tumor (left) and an ATMKO T-cell tumor (right) (original magnification  $\times 40$ ). Images were collected at room temperature using a Zeiss LSM510 META confocal microscope fitted with a 63 $\times$  oil-immersion lens. (B) Quantification of mean nuclear/cytoplasmic intensity ratio for Rel staining shown for 2 B-cell tumors (closed symbols) and 2 T-cell tumors (open symbols) and calculated from 200 images collected for each tumor. (C) Inhibition of ATMKO.CD3 $\epsilon$ KO B-cell tumors (closed symbols) and ATMKO T-cell tumors (open symbols) cocultured with the IKK inhibitors PS1145 (C) or MLN120B (D). (E) quantitative polymerase chain reaction detection of *Malt1* expression in B-cell tumors (B1, B2, and B3) and lipopolysaccharide (LPS)-activated B cells. Data were collected on the ABI 9700 real-time polymerase chain reaction system (Applied Biosystems), and relative expression of *Malt1* was determined using the  $2^{-\Delta\Delta C_T}$  method, normalized to  $\beta$ -actin expression, and presented as fold expression ( $\pm$  standard deviation) relative to LPS-activated B cells. This experiment is representative of 3 independent experiments for each sample. Inhibition of B-cell tumors (closed symbols) and T-cell tumors (open symbols) cocultured with the MALT1 inhibitors Z-VPRPR-fmk (F) or M1-2 (G). For panels C-D and F-G, viable cells were counted and inhibition was calculated as described. Data are representative of 3 independent experiments examining survival of 4 to 6 B-cell tumors and 2 to 4 T-cell tumors in each experiment.

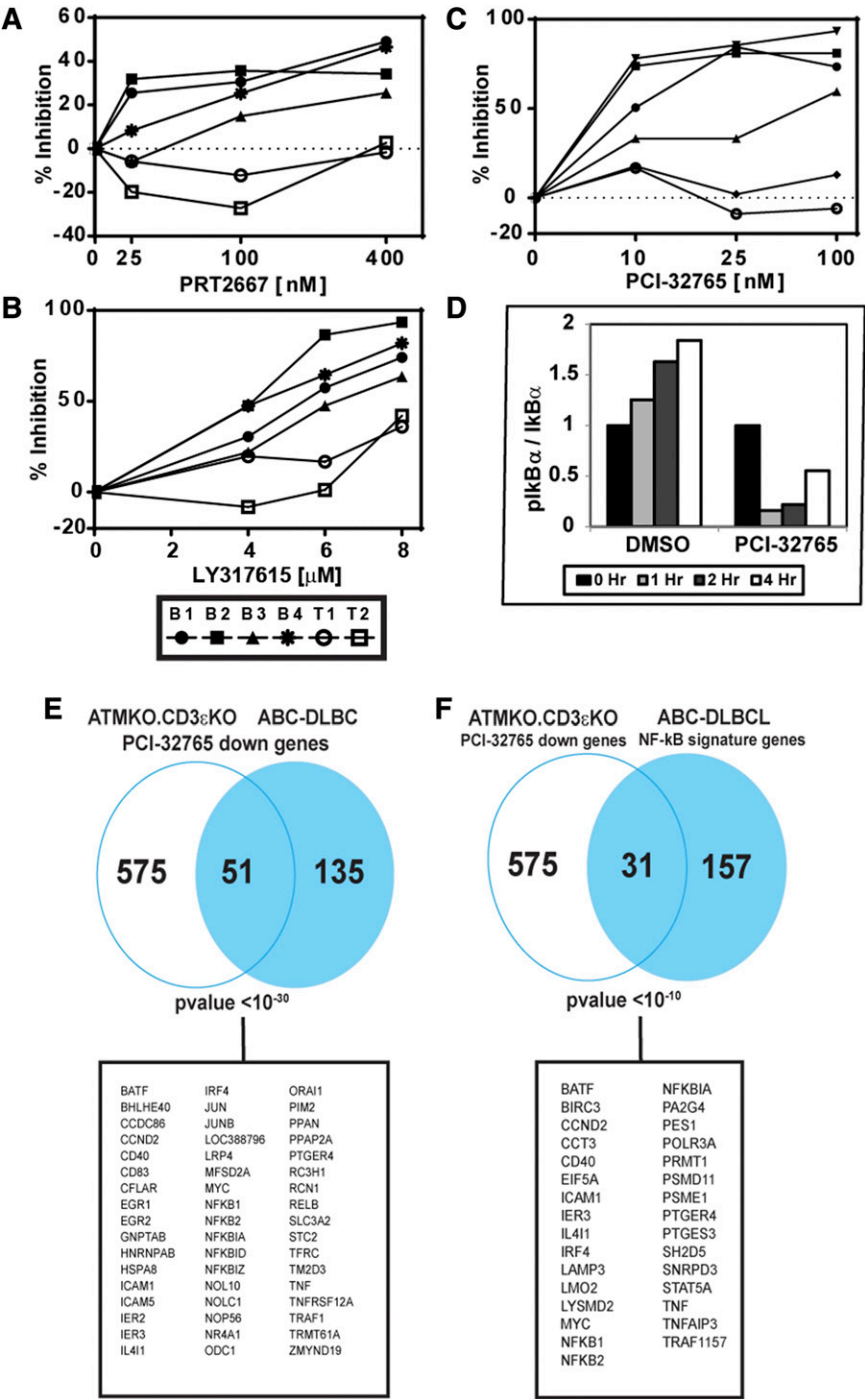
Our study suggests that T cell–dependent immune surveillance is an important mechanism preventing development of B-cell malignancies in the context of ATM deficiency. ATMKO.CD3 $\epsilon$ KO B-cell lymphomas express high levels of MHC and costimulatory molecules that may promote their *in vivo* recognition and elimination by activated T cells. These tumors also express CD95 that may predispose them to apoptosis by FAS ligand–positive T cells, a mechanism recently reported to mediate immune surveillance against some B-cell lymphomas.<sup>56</sup> AIDS patients and immune-suppressed individuals with impaired T-cell function also develop B-cell malignancies with increased frequency, and, in the context of aging-associated decreases in T-cell function, development of ABC DLBCL, but not GCB DLBCL, is substantially elevated in elderly patients.<sup>57–59</sup> The findings reported here provide a model to further assess the mechanisms by which T cells control the emergence of ABC DLBCL.

It is thought that DLBCL derives from GC or post-GC B cells<sup>12</sup> that undergo TD antigen-driven GC differentiation, leading to altered gene expression<sup>8,35</sup> and somatically mutated BCRs.<sup>29,60</sup> The B-cell lymphomas described here develop in the absence of T cells and,

therefore, in the absence of conventional TD GC, yet they resemble GC-experienced cells. They have gene expression profiles similar to post-GC ABC DLBCL and express IgM<sup>+</sup> BCR, with ongoing somatic hypermutation and associated *Aicda* expression. Further, detection of shared IgVH mutations in each cell line suggests that activation, induction of AID, and somatic hypermutation preceded transformation. It is not clear how AID is regulated in these lymphomas; although expressed AID is sufficient to promote ongoing IgVH mutations, it is not sufficient to promote class-switch recombination (CSR), because all lymphomas were IgM<sup>+</sup>. This defect in CSR could result from recombination defects<sup>61</sup> or lack of targeting to switch regions<sup>62</sup> arising from ATM deficiency. Hypermutation independent of GC or T cells has been previously reported.<sup>28,63,64</sup> In this context, ATM-deficient lymphomas resemble memory B cells induced by T-I type 2 polysaccharide antigens, in that they share an unusual CD21<sup>–</sup>CD23<sup>–</sup> phenotype and express BCRs with only low-level IgVH mutations.<sup>28</sup> Therefore, exposure to environmental T-I type 2 antigens, such as *Streptococcus pneumoniae*, occurring in the context of T-cell deficiency may provide critical activation signals that promote B-cell transformation in ATMKO.CD3 $\epsilon$ KO mice and in humans.



**Figure 6. Inhibition of BCR signaling suppresses cell recovery and NF- $\kappa$ B activation in ATMKO.CD3 $\epsilon$ KO B-cell lymphomas.** ATMKO.CD3 $\epsilon$ KO B-cell lymphoma lines (closed symbols) and ATMKO T-cell lymphoma lines (open symbols) were cocultured with titrated amounts of PRT2667 (Syk inhibitor) (A), LY317615 (PKC $\beta$  inhibitor) (B), or PCI-32765 (BTK inhibitor) (C). For panels A-C, viable cells were counted, and inhibition was calculated as described in "Materials and methods." Data are representative of 3 independent experiments examining survival of 4 to 6 B-cell lymphomas and 2 to 4 T-cell lymphomas in each experiment. (D) Inhibition of BTK signaling suppresses NF- $\kappa$ B activation in ATMKO.CD3 $\epsilon$ KO tumors. Lymphoma cells were treated with DMSO or the BTK inhibitor PCI-32765 (100 nM) for the indicated time points and lysed, and sequential western blot analyses were performed to detect p-IkB $\alpha$ , total IkB $\alpha$ , and  $\beta$ -actin expression. Band intensities were quantitated and then normalized to  $\beta$ -actin. NF- $\kappa$ B activation was expressed as the p-IkB $\alpha$ /IkB $\alpha$  ratio at each time point relative to the value at time = 0 hours. Data are representative 3 independent experiments examining NF- $\kappa$ B activation in 2 B-cell lymphomas. Signature analysis comparing genes downregulated in ATMKO.CD3 $\epsilon$ KO tumors (n = 2) treated with PCI-32765 (100 nM; 6 hours at 37°C) to genes downregulated in a human ABC DLBCL cell line similarly treated with PCI-32765 (E) or to an NF- $\kappa$ B signaling signature derived from human ABC DLBCL (F). Genes identified as downregulated in panels E-F were at least 1.3-fold downregulated in  $\geq 50\%$  of the samples analyzed at the 6-hour treatment point. P values for the overlaps and the genes common to both tumors are shown.



NF- $\kappa$ B is a tightly regulated signaling pathway that inhibits apoptosis and promotes cell proliferation. Recent studies demonstrating that human ABC DLBCL depends on constitutive NF- $\kappa$ B activation for survival<sup>11,13</sup> highlight the fact that deregulated NF- $\kappa$ B signaling can promote tumor development.<sup>6,12,65</sup> For some lymphomas, genetic mutations that enhance NF- $\kappa$ B signaling (*CARMA1*, *MyD88*, or BCR) or minimize inhibition of NF- $\kappa$ B signaling (*TNFAIP3*) have been identified,<sup>11,66</sup> but for many other lymphomas, including the ATMKO.CD3 $\epsilon$ KO lymphomas, the mechanisms mediating NF- $\kappa$ B activation are unknown. Although it is unclear whether the mutations leading to constitutive NF- $\kappa$ B activation in human or mouse lymphomas are early transforming events or are

byproducts of transformation, it is clear that NF- $\kappa$ B activation provides them with a survival advantage.

MALT1 is a component of a complex that links BCR signaling to downstream NF- $\kappa$ B activation and plays important roles in normal B-cell biology and in the pathogenesis of human ABC DLBCL.<sup>14,16,39,45</sup> The MMU18 amplicon in ATMKO.CD3 $\epsilon$ KO lymphomas, containing *Malt1*, is orthologous to a region that is amplified in  $>30\%$  of human ABC DLBCL<sup>7,9</sup> and correlates with *Malt1* overexpression in these mouse lymphomas. Despite studies implicating MALT1 in lymphomagenesis, evidence documenting an ability of MALT1 to directly activate NF- $\kappa$ B in the absence BCR signaling or to be itself oncogenic has been difficult to demonstrate.<sup>67-69</sup> Although the mechanism by which

MALT1 contributes to pathogenesis of ATMKO.CD3εKO lymphomas remains to be determined, the ubiquitous expression of amplified *Malt1* in these lymphomas suggests that genomic amplification is an early event in tumor development and that maintenance is important for tumor survival.

This report demonstrates that ATM deficiency profoundly predisposes mice to develop B-cell lymphomas that resemble human ABC DLBCL and that emergence of these tumors occurs only when T cells are absent. This mouse model may be useful for studying both etiology and therapy of ABC DLBCL, as well as the role of T-dependent mechanisms in preventing development of these B-cell lymphomas.

## Acknowledgments

The authors thank Dr Darawalee Wangsa for SKY probes and Drs Ranjan Sen, Joy Williams, Michael Kruhlak, and Elias Campo for helpful discussions.

## References

- Shiloh Y. ATM and related protein kinases: safeguarding genome integrity. *Nat Rev Cancer*. 2003;3(3):155-168.
- Petiniot LK, Weaver Z, Barlow C, et al. Recombinase-activating gene (RAG) 2-mediated V(D)J recombination is not essential for tumorigenesis in Atm-deficient mice. *Proc Natl Acad Sci USA*. 2000;97(12):6664-6669.
- Barlow C, Hirotsune S, Paylor R, et al. Atm-deficient mice: a paradigm of ataxia telangiectasia. *Cell*. 1996;86(1):159-171.
- Sandoval C, Swift M. Treatment of lymphoid malignancies in patients with ataxia-telangiectasia. *Med Pediatr Oncol*. 1998;31(6):491-497.
- Suarez F, Mahlaoui N, Canioni D, et al. Incidence, presentation, and prognosis of malignancies in ataxia-telangiectasia: a report from the French national registry of primary immune deficiencies. *J Clin Oncol*. 2015;33(2):202-208.
- Staudt LM, Dave S. The biology of human lymphoid malignancies revealed by gene expression profiling. *Adv Immunol*. 2005;87:163-208.
- Bea S, Zettl A, Wright G, et al; Lymphoma/Leukemia Molecular Profiling Project. Diffuse large B-cell lymphoma subgroups have distinct genetic profiles that influence tumor biology and improve gene-expression-based survival prediction. *Blood*. 2005;106(9):3183-3190.
- Alizadeh AA, Eisen MB, Davis RE, et al. Distinct types of diffuse large B-cell lymphoma identified by gene expression profiling. *Nature*. 2000;403(6769):503-511.
- Tagawa H, Suguro M, Tsuzuki S, et al. Comparison of genome profiles for identification of distinct subgroups of diffuse large B-cell lymphoma. *Blood*. 2005;106(5):1770-1777.
- Pasqualucci L, Trifonov V, Fabbri G, et al. Analysis of the coding genome of diffuse large B-cell lymphoma. *Nat Genet*. 2011;43(9):830-837.
- Staudt LM. Oncogenic activation of NF-κappaB. *Cold Spring Harb Perspect Biol*. 2010;2(6):a000109.
- Shaffer AL III, Young RM, Staudt LM. Pathogenesis of human B cell lymphomas. *Annu Rev Immunol*. 2012;30:565-610.
- Davis RE, Brown KD, Siebenlist U, Staudt LM. Constitutive nuclear factor kappaB activity is required for survival of activated B cell-like diffuse large B cell lymphoma cells. *J Exp Med*. 2001;194(12):1861-1874.
- Ferch U, Kloos B, Gewies A, et al. Inhibition of MALT1 protease activity is selectively toxic for activated B cell-like diffuse large B cell lymphoma cells. *J Exp Med*. 2009;206(11):2313-2320.
- Uren AG, O'Rourke K, Aravind LA, et al. Identification of paracaspases and metacaspases: two ancient families of caspase-like proteins, one of which plays a key role in MALT lymphoma. *Mol Cell*. 2000;6(4):961-967.
- Hailfinger S, Lenz G, Ngo V, et al. Essential role of MALT1 protease activity in activated B cell-like diffuse large B-cell lymphoma. *Proc Natl Acad Sci USA*. 2009;106(47):19946-19951.
- Lam KP, Kühn R, Rajewsky K. In vivo ablation of surface immunoglobulin on mature B cells by inducible gene targeting results in rapid cell death. *Cell*. 1997;90(6):1073-1083.
- Sommers CL, Dejarnette JB, Huang K, et al. Function of CD3ε-mediated signals in T cell development. *J Exp Med*. 2000;192(6):913-919.
- Muramatsu M, Kinoshita K, Fagarasan S, Yamada S, Shinkai Y, Honjo T. Class switch recombination and hypermutation require activation-induced cytidine deaminase (AID), a potential RNA editing enzyme. *Cell*. 2000;102(5):553-563.
- Shin DM, Shaffer DJ, Wang H, Roopenian DC, Morse HC III. NOTCH is part of the transcriptional network regulating cell growth and survival in mouse plasmacytomas. *Cancer Res*. 2008;68(22):9202-9211.
- Edgar R, Domrachev M, Lash AE. Gene Expression Omnibus: NCBI gene expression and hybridization array data repository. *Nucleic Acids Res*. 2002;30(1):207-210.
- Padilla-Nash HM, Barenboim-Stapleton L, Difilippantonio MJ, Ried T. Spectral karyotyping analysis of human and mouse chromosomes. *Nat Protoc*. 2007;1(6):3129-3142.
- Liyanage M, Coleman A, du Manoir S, et al. Multicolour spectral karyotyping of mouse chromosomes. *Nat Genet*. 1996;14(3):312-315.
- Padilla-Nash HM, Hathcock K, McNeil NE, et al. Spontaneous transformation of murine epithelial cells requires the early acquisition of specific chromosomal aneuploidies and genomic imbalances. *Genes Chromosomes Cancer*. 2012;51(4):353-374.
- Camps J, Grade M, Nguyen QT, et al. Chromosomal breakpoints in primary colon cancer cluster at sites of structural variants in the genome. *Cancer Res*. 2008;68(5):1284-1295.
- Chiang YJ, Jordan MS, Horai R, Schwartzberg PL, Koretzky GA, Hodes RJ. Cbl enforces an SLP76-dependent signaling pathway for T cell differentiation. *J Biol Chem*. 2009;284(7):4429-4438.
- Morse HC III, Anver MR, Fredrickson TN, et al; Hematopathology subcommittee of the Mouse Models of Human Cancers Consortium. Bethesda proposals for classification of lymphoid neoplasms in mice. *Blood*. 2002;100(1):246-258.
- Obukhanych TV, Nussenzweig MC. T-independent type II immune responses generate memory B cells. *J Exp Med*. 2006;203(2):305-310.
- Maul RW, Gearhart PJ. AID and somatic hypermutation. *Adv Immunol*. 2010;105:159-191.
- Liu M, Schatz DG. Balancing AID and DNA repair during somatic hypermutation. *Trends Immunol*. 2009;30(4):173-181.
- Robbiani DF, Bunting S, Feldhahn N, et al. AID produces DNA double-strand breaks in non-Ig genes and mature B cell lymphomas with reciprocal chromosome translocations. *Mol Cell*. 2009;36(4):631-641.
- Okazaki IM, Kotani A, Honjo T. Role of AID in tumorigenesis. *Adv Immunol*. 2007;94:245-273.
- Pasqualucci L, Bhagat G, Jankovic M, et al. AID is required for germinal center-derived lymphomagenesis. *Nat Genet*. 2008;40(1):108-112.
- Hathcock KS, Laszlo G, Pucillo C, Linsley P, Hodes RJ. Comparative analysis of B7-1 and B7-2 costimulatory ligands: expression and function. *J Exp Med*. 1994;180(2):631-640.
- Shaffer AL, Wright G, Yang L, et al. A library of gene expression signatures to illuminate normal and pathological lymphoid biology. *Immunol Rev*. 2006;210(1):67-85.
- Shaffer AL, Rosenwald A, Hurt EM, et al. Signatures of the immune response. *Immunity*. 2001;15(3):375-385.
- Yang Y, Shaffer AL III, Emre NC, et al. Exploiting synthetic lethality for the therapy of ABC diffuse

## Authorship

Contribution: K.S.H. designed the research, performed the research, analyzed the data, and wrote the paper; H.M.P.-N., J.C., D.T., A.L.S., and H.C.M. designed the research, performed the research, analyzed the data, and edited the paper; D.-M.S. and S.M.S. analyzed the data; R.W.M. designed the research, performed the research, and analyzed the data; and P.J.G., L.M.S., T.R., and R.J.H. designed the research and edited the paper.

Conflict-of-interest disclosure: The authors declare no competing financial interests.

Correspondence: Richard J. Hodes, 10 Center Dr, Room 4B05, National Cancer Institute, National Institutes of Health, Bethesda, MD 20892; e-mail: richard\_hodes@nih.gov.

- large B cell lymphoma. *Cancer Cell*. 2012;21(6):723-737.
38. Beroukhi R, Getz G, Nghiemphu L, et al. Assessing the significance of chromosomal aberrations in cancer: methodology and application to glioma. *Proc Natl Acad Sci USA*. 2007;104(50):20007-20012.
  39. Thome M, Charton JE, Pelzer C, Hailfinger S. Antigen receptor signaling to NF-kappaB via CARMA1, BCL10, and MALT1. *Cold Spring Harb Perspect Biol*. 2010;2(9):a003004.
  40. Blonska M, Lin X. NF-kB signaling pathways regulated by CARMA family of scaffold proteins. *Cell Res*. 2011;21(1):55-70.
  41. Gilmore TD, Kalaitzidis D, Liang MC, Starczynowski DT. The c-Rel transcription factor and B-cell proliferation: a deal with the devil. *Oncogene*. 2004;23(13):2275-2286.
  42. Lam LT, Davis RE, Pierce J, et al. Small molecule inhibitors of IkappaB kinase are selectively toxic for subgroups of diffuse large B-cell lymphoma defined by gene expression profiling. *Clin Cancer Res*. 2005;11(1):28-40.
  43. Hideshima T, Neri P, Tassone P, et al. MLN120B, a novel IkappaB kinase beta inhibitor, blocks multiple myeloma cell growth in vitro and in vivo. *Clin Cancer Res*. 2006;12(19):5887-5894.
  44. Fontan L, Yang C, Kabaleeswaran V, et al. MALT1 small molecule inhibitors specifically suppress ABC-DLBCL in vitro and in vivo. *Cancer Cell*. 2012;22(6):812-824.
  45. Kaileh M, Sen R. NF-kB function in B lymphocytes. *Immunol Rev*. 2012;246(1):254-271.
  46. Rickert RC. New insights into pre-BCR and BCR signalling with relevance to B cell malignancies. *Nat Rev Immunol*. 2013;13(8):578-591.
  47. Davis RE, Ngo VN, Lenz G, et al. Chronic active B-cell-receptor signalling in diffuse large B-cell lymphoma. *Nature*. 2010;463(7277):88-92.
  48. Yang G, Zhou Y, Liu X, et al. A mutation in MYD88 (L265P) supports the survival of lymphoplasmacytic cells by activation of Bruton tyrosine kinase in Waldenström macroglobulinemia. *Blood*. 2013;122(7):1222-1232.
  49. Boulton J. Ataxia telangiectasia gene mutations in leukaemia and lymphoma. *J Clin Pathol*. 2001;54(7):512-516.
  50. Cuneo A, Bigoni R, Rigolin GM, et al. Acquired chromosome 11q deletion involving the ataxia telangiectasia locus in B-cell non-Hodgkin's lymphoma: correlation with clinicobiologic features. *J Clin Oncol*. 2000;18(13):2607-2614.
  51. Zhu Y, Monni O, Franssila K, et al. Deletions at 11q23 in different lymphoma subtypes. *Haematologica*. 2000;85(9):908-912.
  52. Grønbaek K, Worm J, Ralfkiaer E, Ahrenkiel V, Hokland P, Guldberg P. ATM mutations are associated with inactivation of the ARF-TP53 tumor suppressor pathway in diffuse large B-cell lymphoma. *Blood*. 2002;100(4):1430-1437.
  53. Stankovic T, Stewart GS, Byrd P, Fegan C, Moss PA, Taylor AM. ATM mutations in sporadic lymphoid tumours. *Leuk Lymphoma*. 2002;43(8):1563-1571.
  54. Starostik P, Manshouri T, O'Brien S, et al. Deficiency of the ATM protein expression defines an aggressive subgroup of B-cell chronic lymphocytic leukemia. *Cancer Res*. 1998;58(20):4552-4557.
  55. Schaffner C, Idler I, Stiglbauer S, Döhner H, Lichter P. Mantle cell lymphoma is characterized by inactivation of the ATM gene. *Proc Natl Acad Sci USA*. 2000;97(6):2773-2778.
  56. Afshar-Sterle S, Zotos D, Bernard NJ, et al. Fas ligand-mediated immune surveillance by T cells is essential for the control of spontaneous B cell lymphomas. *Nat Med*. 2014;20(3):283-290.
  57. de Visser KE, Eichten A, Coussens LM. Paradoxical roles of the immune system during cancer development. *Nat Rev Cancer*. 2006;6(1):24-37.
  58. Brady G, MacArthur GJ, Farrell PJ. Epstein-Barr virus and Burkitt lymphoma. *J Clin Pathol*. 2007;60(12):1397-1402.
  59. Mareschal S, Lanic H, Ruminy P, Bastard C, Tilly H, Jardin F. The proportion of activated B-cell like subtype among de novo diffuse large B-cell lymphoma increases with age. *Haematologica*. 2011;96(12):1888-1890.
  60. Klein U, Dalla-Favera R. Germinal centres: role in B-cell physiology and malignancy. *Nat Rev Immunol*. 2008;8(1):22-33.
  61. Lumsden JM, McCarty T, Petiniot LK, et al. Immunoglobulin class switch recombination is impaired in Atm-deficient mice. *J Exp Med*. 2004;200(9):1111-1121.
  62. Stavnezer J, Guikema JE, Schrader CE. Mechanism and regulation of class switch recombination. *Annu Rev Immunol*. 2008;26:261-292.
  63. Toellner KM, Jenkinson WE, Taylor DR, et al. Low-level hypermutation in T cell-independent germinal centers compared with high mutation rates associated with T cell-dependent germinal centers. *J Exp Med*. 2002;195(3):383-389.
  64. William J, Euler C, Christensen S, Shlomchik MJ. Evolution of autoantibody responses via somatic hypermutation outside of germinal centers. *Science*. 2002;297(5589):2066-2070.
  65. Küppers R. Mechanisms of B-cell lymphoma pathogenesis. *Nat Rev Cancer*. 2005;5(4):251-262.
  66. Compagno M, Lim WK, Grunn A, et al. Mutations of multiple genes cause deregulation of NF-kappaB in diffuse large B-cell lymphoma. *Nature*. 2009;459(7247):717-721.
  67. Li Z, Wang H, Xue L, et al. Emu-BCL10 mice exhibit constitutive activation of both canonical and noncanonical NF-kappaB pathways generating marginal zone (MZ) B-cell expansion as a precursor to splenic MZ lymphoma. *Blood*. 2009;114(19):4158-4168.
  68. Vicente-Dueñas C, Fontán L, Gonzalez-Herrero I, et al. Expression of MALT1 oncogene in hematopoietic stem/progenitor cells recapitulates the pathogenesis of human lymphoma in mice. *Proc Natl Acad Sci USA*. 2012;109(26):10534-10539.
  69. Ho L, Davis RE, Conne B, et al. MALT1 and the API2-MALT1 fusion act between CD40 and IKK and confer NF-kappa B-dependent proliferative advantage and resistance against FAS-induced cell death in B cells. *Blood*. 2005;105(7):2891-2899.